Continuous-wave Raman laser pumped within a semiconductor disk laser cavity

Daniele C. Parrotta,* Walter Lubeigt, Alan J. Kemp, David Burns, Martin D. Dawson, and Jennifer E. Hastie

Institute of Photonics, SUPA, University of Strathclyde, Wolfson Centre, 106 Rottenrow, Glasgow G4 0NW, UK

**Corresponding author: daniele.parrotta@strath.ac.uk*

Received January 21, 2011; revised February 22, 2011; accepted February 22, 2011; posted February 25, 2011 (Doc. ID 141410); published March 18, 2011

A $KGd(WO_4)_2$ Raman laser was pumped within the cavity of a cw diode-pumped InGaAs semiconductor disk laser (SDL). The Raman laser threshold was reached for 5.6 W of absorbed diode pump power, and output power up to 0.8 W at 1143 nm, with optical conversion efficiency of 7.5% with respect to the absorbed diode pump power, was demonstrated. Tuning the SDL resulted in tuning of the Raman laser output between 1133 and 1157 nm. © 2011 Optical Society of America

OCIS codes: 140.3550, 140.3580, 140.3600, 140.7270.

There has recently been great interest in cw Raman lasers, which use stimulated Raman scattering (SRS) to extend the wavelength coverage of solid-state lasers. The first cw crystalline Raman laser used $Ba(NO_3)_2$ in an external resonator [1]. Since then, several efficient cw Raman lasers pumped within solid-state laser cavities have been demonstrated, giving access to the 1.1–1.5 μm spectral region with thresholds of a few watts or less [2–4]. In contrast to optical parametric oscillators (OPOs) [5], the wavelength (Stokes) shift is fixed by the properties of the Raman crystal; therefore, a tunable Raman laser requires a tunable pump source. For this reason, with the exception of fiber lasers, cw solid-state Raman lasers are not usually tunable.

Here we demonstrate that semiconductor disk lasers (SDLs) are attractive alternative pump sources for intracavity Raman lasers. SDLs, also known as vertical external cavity surface-emitting lasers, consist of a semiconductor platelet gain-and-mirror structure, optically pumped within a high-finesse external resonator [6]. Bandgap engineering of the gain structure in a variety of III–V alloys provides broad spectral coverage from the visible to the mid-IR. SDLs are broadly tunable (~16 nm in the red [7] to >100 nm in the mid-IR [8]) about any particular central wavelength. Moreover, their high intracavity fields and short carrier lifetimes (approximately nanoseconds) are well suited to low-noise, intracavity nonlinear conversion: e.g., frequency-doubling [7] and intracavity-pumping of OPOs [9]. Thus utilizing SDLs as intracavity pump sources for cw Raman lasers offers exciting prospects for both extended tunable operation and coverage of novel wavelength regions.

Here, as a first demonstration of this capability, we report a cw Raman laser pumped within a 1060 nm wavelength InGaAs SDL. The Raman laser, which utilizes $KGd(WO_4)_2$ (KGW) as the Raman gain medium, is tunable between 1133 and 1157 nm and produces output powers of up to 0.8 W. Although SDLs can be designed to operate around 1150 nm without nonlinear conversion, this demonstration proves the principle of our general approach, and in this specific case it removes the need for the highly strained gain structures required to directly generate these wavelengths.

The SDL gain structure was designed to operate around 1060 nm, and contained fifteen 7 nm thick strain-compensated $In_{0.28}Ga_{0.72}As$ quantum wells separated by $GaAs/GaAs_{0.9}P_{0.1}/GaAs$ barrier layers, monolithically grown on a distributed Bragg reflector (DBR) consisting of 35 pairs of $AlAs/Al_{0.2}Ga_{0.8}As$ $\lambda/4$ layers. The structure was completed by an $Al_{0.3}Ga_{0.7}As$ window layer and a GaAs capping layer. For effective thermal management, an uncoated, plane–parallel synthetic single-crystal diamond heat spreader, 500 μm thick, was bonded onto the intracavity surface of the SDL chip via liquid-assisted optical contacting [10]. This structure was clamped in a water-cooled brass mount (water temperature of 7 °C) with 100 μm thick indium foil at the interfaces. The SDL chip was optically pumped by an 808 nm fiber-coupled diode laser (100 μm core diameter, 0.22 NA) with a pump waist radius of ~45 μm. High-power operation (>1 W) and broad tunability of such an SDL are described elsewhere [11].

Previously employed in cw Raman lasers [2–4], KGW has relatively high Raman gain (~6 cm/GW), acceptable thermal conductivity (~3 W/mK), and a high optical damage threshold (~10 GW/cm^2) [12]. The 30 mm long KGW crystal (EKSMA Optics) was cut for propagation along the Np axis, with both end faces antireflection coated for 1040–1190 nm ($R < 0.1\%$). Depending on the crystal orientation with respect to the pump polarization, Np-cut KGW can exhibit two different dominant Stokes shifts: 767 cm^{-1} and 901 cm^{-1}, respectively [12].

The four-mirror Raman resonator was aligned within a four-mirror SDL cavity with two mirrors in common (Fig. 1). Each curved mirror had a radius of curvature of 100 mm and was highly reflective ($R \sim 99.98\%$) from 1000 to 1155 nm. As the SDL high-reflectivity DBR stop

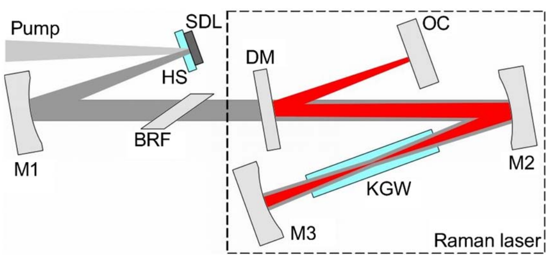

Fig. 1. (Color online) Schematic of the KGW Raman laser pumped within an InGaAs SDL: HS, diamond heat spreader; M1–M3, high reflectors; DM, dichroic mirror; OC, output coupler; and BRF, birefringent filter.

0146-9592/11/071083-03$15.00/0

band was not spectrally broad enough to reflect the Stokes shifted light, a planar dichroic mirror (DM) with high transmission for the SDL wavelength range ($R < 1\%$, 1030–1080 nm) and high reflectivity for the Raman laser ($R > 99.98\%$, >1140 nm) was required (tilt angle ~2°). The SDL cavity was aligned to match the radius of the fundamental mode to the laser diode pump spot at the SDL chip and to produce a calculated ~31 μm fundamental cavity mode waist radius in the KGW: the cavity arm lengths were SDL–M1, 50 mm; M1–M2, 550 mm; M2–KGW, 46 mm; and KGW–M3, 93 mm. The distance between the output coupler (OC), and the DM was adjusted so that the calculated Raman laser fundamental mode radius in the KGW was also ~31 μm: DM–OC, 175 mm and DM–M2, 305 mm. The actual beam waists were somewhat larger due to multitransverse mode operation. Wavelength selection and tuning of the SDL were performed using a 4 mm thick quartz birefringent filter (BRF) at Brewster's angle in the SDL cavity arm. The KGW crystal, held in a water-cooled brass mount (water temperature of 7 °C), was oriented to give a Raman shift of 767 cm^{-1}.

The power transfer characteristic of the cw Raman laser is shown in Fig. 2 for an OC transmission of 0.8%. The Raman laser threshold was reached for an absorbed diode laser input power of 5.6 W, with stable Raman conversion observed for the 8–11.5 W range. The instability just above the threshold is due, we believe, to interaction between higher order transverse modes gradually reaching the threshold. The slope efficiency with respect to the absorbed diode pump power in the stable range was 22%. The maximum output power of 0.8 W at 1143 nm was achieved for 10.7 W input power: an optical conversion efficiency of 7.5%, in line with previously reported values for cw Raman lasers (e.g., [4]). The SDL intracavity power was monitored via the leakage signal through M1 and estimated using the measured reflectivity of this mirror. At the Raman laser threshold, the SDL intracavity power was ~90 ± 11 W; during stable operation, it was around 115 ± 14 W, increasing slowly with pump power. Thermal rollover [6] of both the SDL and Raman laser fields occurred for absorbed diode laser powers >11 W. Rollover of the SDL intracavity field is slow initially due to reduced losses to the Raman laser.

During Raman conversion, the SDL beam propagation factors were measured to be $M^2_{\text{horizontal}} = 4.65$ and $M^2_{\text{vertical}} = 4.85$. This relatively poor beam quality results, we believe, from the interaction of three factors. First, the heat induced by SRS generates an aberrated thermal lens. Second, the losses associated with preferential Raman conversion of lower order transverse modes favor SDL oscillation on higher order transverse modes. Last, small adjustments to the alignment of the pump optics for high-power operation tend to result in a larger pump spot radius favoring operation on higher order transverse modes [13]. However, Raman conversion is typically accompanied by "beam clean-up" [14], and indeed the beam propagation factors of the Raman laser were measured to be $M^2_{\text{horizontal}} = 2.5$ and $M^2_{\text{vertical}} = 2.55$.

The Raman laser polarization was tilted by ~15° with respect to the horizontally polarized SDL beam. The polarization of the SDL beam is effectively constrained by the Brewster surfaces; however, the Stokes field is not. The fact that the Raman laser oscillates with a tilted polarization may indicate that the Raman gain for the 767 cm^{-1} Stokes shift is higher at this angle. The mounting arrangements precluded rotation of the KGW and hence a detailed investigation of this effect.

Rotating the BRF resulted in tuning of the SDL and hence the Raman laser, as shown in Fig. 3 for an absorbed diode laser input power of 10.7 W. The Raman laser operated over the range 1133.5–1157 nm (SDL range 1043–1063 nm), but tuning was not continuous. Insertion of the KGW caused modulation of the tuning curve of the SDL. This is consistent with the combined effects of the etalon formed by the diamond heat spreader and the birefringent filtering that would be introduced if the SDL polarization were slightly misaligned from the Ng axis of the KGW [15]. This variation in the intracavity pump power meant that the Raman laser operated at discrete wavelengths corresponding to the maxima of the modulation, with peak separation of ~5 nm. (The free spectral range of the diamond heat spreader is ~0.5 nm.)

Using a smaller output coupling, we were able to observe the cascaded Raman conversion: a second spectral

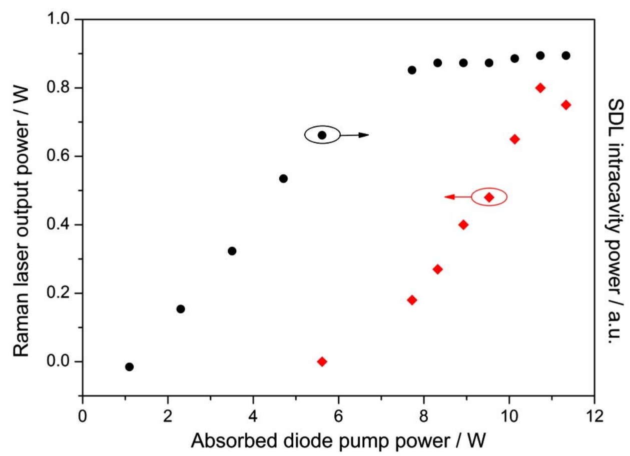

Fig. 2. (Color online) Power transfer characteristics of the cw KGW Raman laser, including the SDL intracavity power measured via signal leakage through M1.

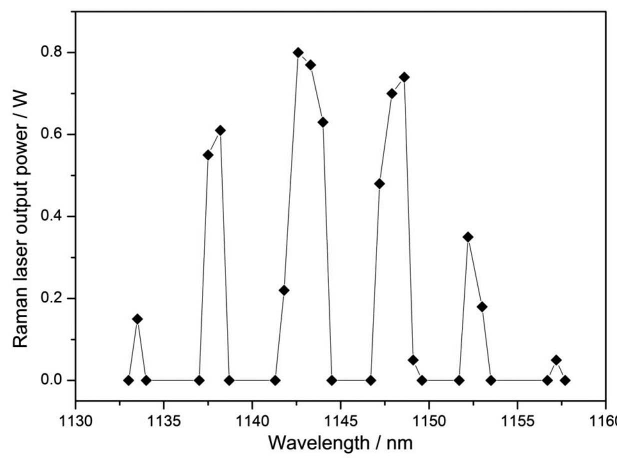

Fig. 3. Tuning of the Raman laser via rotation of the intracavity BRF. The measurement occurred at an absorbed diode laser input power of 10.7 W.

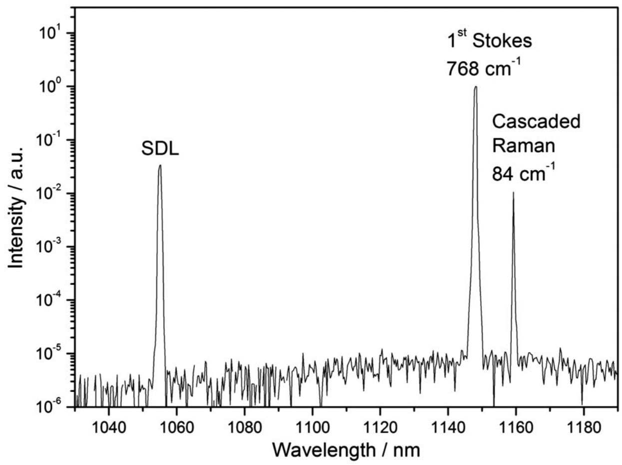

Fig. 4. Emission spectrum of the laser displaying cascaded Raman conversion with smaller output coupling.

peak, just within the high-reflectivity band of the Raman laser mirrors, corresponding to a further 84 cm^{-1} shift of the 1143 nm field, which had an estimated intracavity power >100 W. The 84 cm^{-1} Stokes shift in KGW is observed for this crystal orientation in [12], although the Raman gain is not measured. Cascaded Raman conversion in a cw intracavity Raman laser has only been reported once previously to our knowledge [16]. This second peak was observed at discrete wavelengths over a 9 nm range, 1150–1159 nm, and a typical output spectrum is shown in Fig. 4, measured using an optical spectrum analyzer with 0.3 nm resolution. An 84 cm^{-1} shift of the SDL wavelength is not observed, as this would be transmitted by the DM and hence filtered out by the BRF. The demonstration of cascaded Raman conversion of an SDL has the potential to further extend the wavelength coverage of these lasers. Cascaded Raman conversion in KGW via a second 767 cm^{-1} Stokes shift to reach wavelengths up to ~1270 nm might be possible with appropriate cavity mirrors. The high intracavity power at the Stokes wavelength also offers the prospect of frequency-doubling to the yellow, as previously demonstrated for other Raman lasers in e.g., [4].

In conclusion, for the first time to our knowledge, a Raman laser has been pumped by a SDL. The cw, KGW Raman laser, pumped within an InGaAs SDL, achieved output power up to 0.8 W, optical conversion efficiency of 7.5%, and >20 nm spectral coverage from 1133 to 1157 nm. Other SDL gain structures, in combination with a variety of crystalline Raman media, have the potential to address the remaining gaps in SDL spectral coverage, e.g., high-power red SDLs [7] shifted to wavelengths of >700 nm.

This work was supported by the Engineering and Physical Sciences Research Council (EPSRC), UK, under grant EP/G00014X.

References

1. S. Grabtchikov, V. A. Lisinetskii, V. A. Orlovich, M. Schmitt, R. Maksimenka, and W. Kiefer, Opt. Lett. **29**, 2524 (2004).
2. A. A. Demidovich, A. S. Grabtchikov, V. A. Lisinetskii, V. N. Burakevich, V. A. Orlovich, and W. Kiefer, Opt. Lett. **30**, 1701 (2005).
3. H. M. Pask, Opt. Lett. **30**, 2454 (2005).
4. P. Dekker, H. M. Pask, and J. A. Piper, Opt. Lett. **32**, 1114 (2007).
5. S. T. Yang, R. C. Eckardt, and R. L. Byer, J. Opt. Soc. Am. B **10**, 1684 (1993).
6. A. C. Tropper, H. D. Foreman, A. Garnache, K. G. Wilcox, and S. Hoogland, J. Phys. D **37**, R75 (2004).
7. S. Calvez, J. E. Hastie, M. Guina, O. G. Okhotnikov, and M. D. Dawson, Laser Photon. Rev. **3**, 407 (2009).
8. D. Burns, J.-M. Hopkins, A. J. Kemp, B. Rösener, N. Schulz, C. Manz, K. Köhler, M. Rattunde, and J. Wagner, Proc. SPIE **7193**, 11 (2009).
9. D. J. M. Stothard, J.-M. Hopkins, D. Burns, and M. H. Dunn, Opt. Express **17**, 10648 (2009).
10. A. J. Kemp, G. J. Valentine, J. M. Hopkins, J. E. Hastie, S. A. Smith, S. Calvez, M. D. Dawson, and D. Burns, IEEE J. Quantum Electron. **41**, 148 (2005).
11. A. J. Maclean, A. J. Kemp, S. Calvez, J. Y. Kim, T. Kim, M. D. Dawson, and D. Burns, IEEE J. Quantum Electron. **44**, 216 (2008).
12. I. V. Mochalov, Opt. Eng. **36**, 1660 (1997).
13. A. J. Maclean, R. B. Birch, P. W. Roth, A. J. Kemp, and D. Burns, J. Opt. Soc. Am. B **26**, 2228 (2009).
14. J. T. Murray, W. L. Austin, and R. C. Powell, Opt. Mater. **11**, 353 (1999).
15. A. J. Kemp, G. J. Friel, T. K. Lake, R. S. Conroy, and B. D. Sinclair, IEEE J. Quantum Electron. **36**, 228 (2000).
16. A. J. Lee, J. Lin, and H. M. Pask, Opt. Lett. **35**, 3000 (2010).